2023-01-0109 Published 11 Apr 2023

Actively Articulated Wheeled Architectures for Autonomous Ground Vehicles - Opportunities and Challenges

Dhruv Mehta, Krishna Chaitanya Kosaraju, and Venkat N Krovi Clemson University

Citation: Mehta, D., Kosaraju, K.C., and Krovi, V.N., "Actively Articulated Wheeled Architectures for Autonomous Ground Vehicles - Opportunities and Challenges," SAE Technical Paper 2023-01-0109, 2023, doi:10.4271/2023-01-0109.

Received: 25 Oct 2022 Revised: 10 Jan 2023 Accepted: 18 Jan 2023

Abstract

Traditional ground vehicle architectures comprise of a chassis connected via passive, semi-active, or active suspension systems to multiple ground wheels. Current design-optimizations of vehicle architectures for on-road applications have diminished their mobility and maneuverability in off-road settings. Autonomous Ground Vehicles (AGV) traversing off-road environments face numerous challenges concerning terrain roughness, soil hardness, uneven obstacle-filled terrain, and varying traction conditions. Numerous Active Articulated-Wheeled (AAW) vehicle architectures have emerged to permit AGVs to adapt to variable terrain conditions in various off-road application arenas (off-road, construction, mining, and space robotics). However, a comprehensive framework of AAW platforms for exploring various facets of system architecture/design, analysis (kinematics/dynamics), and control (motions/forces) remains challenging. While current literature on the AAW system incorporates modeling and control from the legged and wheeled-legged robots community, it lacks a systematic process of architecture selection and motion control that should be developed around critical quantifiable performance parameters. This paper will: (i) analyze a broad body of literature; and (ii) identify modeling and control techniques that can enable the efficient development of AAW platforms. We then analyze key performance measures with respect to traversability, maneuverability, and terrainability, along with an experimental simulation of an AAW vehicle traversing over uneven terrain and how active articulation could achieve some of the critical performance measures. Against the performance parameters, gaps within the existing literature and opportunities for further research are identified to potentially enhance AAW platforms' performance.

Introduction

Next-generation off-road ground vehicles require significantly enhanced mobility and maneuverability to traverse through diverse unstructured terrain conditions. Over the years, tracked vehicles have proven to be a preferred choice in an off-road environment, especially when the vehicle weight exceeds 20 tons and it spends more than 60% of its time in an off-road environment [1]. However, tracked vehicles are slower, consume more energy and require greater maintenance than wheeled vehicles.

For an autonomous off-road vehicle, reliable localization, obstacle avoidance, and map building are critical [2]. Achieving efficient terrain adaptability and obstacle avoidance with higher confidence, change in the conventional structure is one of the potential solutions to enhance its locomotion performance [3]. The conventional architecture change motivates the designing and development of Actively Articulated Wheeled (AAW) Vehicles. AAW vehicles can be predominantly seen in the off-road vehicles space like Multi-functional Utility/Logistics and Equipment vehicles (MULE) as shown in Fig. 1 and the DARPA groundx vehicle shown in Fig. 2. Both have six and four independent active suspensions, respectively. The additional degrees of freedom between the chassis and the wheels can enable the vehicle to adapt and change internal configuration while locomoting through rough terrain. Such *hybrid locomotion* capability could be used to enhance stability, traction and other performance criteria, but would require simultaneous control of the ground-wheels and the active articulation.

At the same time, the additional degrees of freedom increase system complexity and creates challenges for path planning and control. Fortunately, redundancy resolution methods developed for the wheeled-legged robotics community have matured and aid the development of planning and control algorithms [4]. Additionally, down-selecting the optimal design and system architecture depends on mission objectives that motivate the need to understand various quantifiable performance measures described in the Quantifiable

FIGURE 1 Multifunctional Utility and Logistics Equipment Vehicle (MULE) by Lockheed Martin

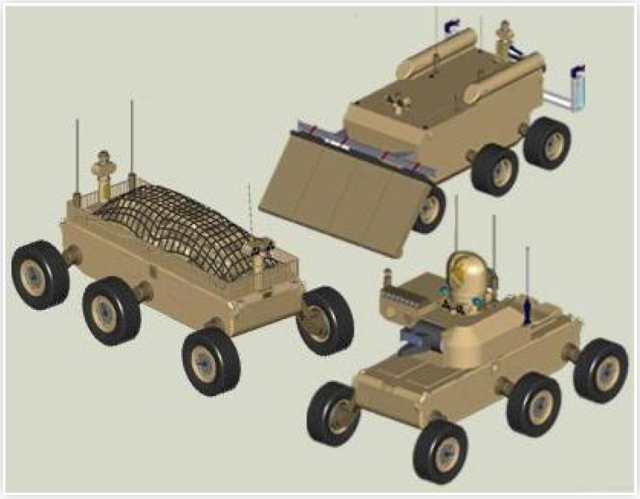

FIGURE 2 DARPA GroundX Vehicle Program

Performance Parameters section. This paper will review the standard planning and control techniques and performance measures that should be incorporated for optimal design and system architecture selection. Further, this manuscript examines the need to develop a unifying design, analysis and control framework, exploit redundancy and understand multi-mode active reconfiguration.

Model Formulation

AAW vehicle is a complex system due to numerous actively articulated links attached to the main body, each of which has a wheel [5]. Accurately commanding the intended trajectory, transmitting the stance of the wheels, and avoiding slip through proper maneuvering, a motion model of the vehicle is necessary [5]. The kinematic model would form the basis for control and integrate the non-holonomic constraints.

Kinematic Modeling

An AAW vehicle can be generalized as having a chassis and wheels attached by n links (active suspensions). In Fig. 3,

FIGURE 3 Generalised AAW vehicle kinematic model

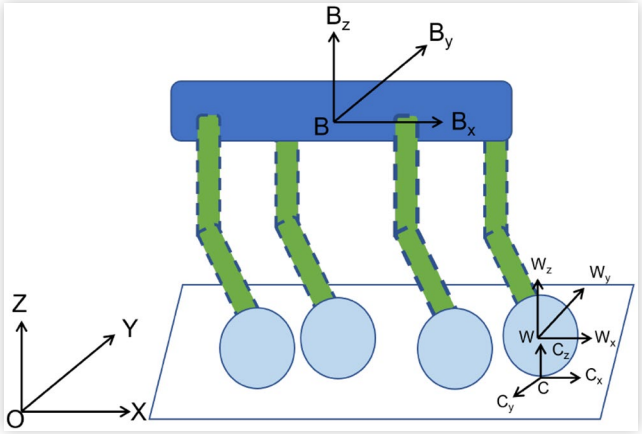

we represent a generalized AAW vehicle kinematic model [6]. It consists of a body frame B (attached to the center of mass of the chassis), wheel axle frame W, contact frame C and the world frame O. Dashed lines show that 'n' links can be modeled between the chassis and the wheel. Wheel is modeled as a rigid disc. The vehicle's configuration can be represented as [x y z $\phi\ \theta\ \psi$] where [x y z] are the positions of the center of mass and [$\phi\ \theta\ \psi$] are the roll, pitch and yaw angles of the center of mass, respectively. A kinematic model can be represented as a sparse matrix shown in Eq. 1 [4, 5].

$$[A]\begin{bmatrix}\dot{x}\\ \dot{y}\\ \dot{z}\\ \dot{\phi}\\ \dot{\theta}\\ \dot{\psi}\end{bmatrix} = J\begin{bmatrix}\dot{\theta}_1\\ \dot{\theta}_2\\ \cdot\\ \cdot\\ :\\ \theta_m\\ \dot{\phi}\end{bmatrix} \tag{1}$$

Eq.1 can be written in its compact form as shown in Eq. 2

$$A\dot{X}_b = J_{\dot{q}} \tag{2}$$

where $J \in \mathbb{R}^{6\times n}$ is the Jacobian matrix that maps vehicle's cartesian space to the joint space, $\dot{X}_b \in \mathbb{R}^{6\times 1}$ is the twist of the chassis center of mass in terms of its linear and angular velocities. $A \in \mathbb{R}^{6\times 6}$ is obtained by by applying the non-holonomic constraint due to the wheels, to the contact twist as shown in Eq. 6, and $\dot{q} \in \mathbb{R}^{n\times 1}$ is a vector that consists of m joints from chassis to the wheels and wheel joint velocities $\dot{\phi}$. Where n is the total number of joints including the wheel joints.

In order to apply pure rolling constraint following wrench basis matrix is formulated

$$\left[S^{\top}\right]_{3\times 6}{}^{C}\left[{}^{O}V_{C}\right]_{6\times 1} = [0\,0\,0]^{\top} \tag{3}$$

where $[S_{6\times 3}]$ is a wrench basis matrix directs the direction in which force is exerted. It prohibits translational motion at contact point by selecting first three rows of the twist vector.

$$S = \begin{bmatrix} I_{3\times3} \\ 0_{3\times3} \end{bmatrix} \tag{4}$$

$C[{}^{O}V_C]$ is the contact frame C velocity obtained from summation of body twists and all the joint twists.

$$ {}^{C}\left[{}^{O}V_C\right] = {}^{C}Ad_B.{}^{B}\left[{}^{F}V_B\right] \tag{5}$$

$$\underbrace{S^{\top}\left[{}^{C}Ad_B\right]}_{A}.{}^{B}\left[{}^{F}V_B\right] = J\dot{q} \tag{6}$$

where ${}^{B}\left[{}^{F}V_B\right] = \dot{X}_b$ and ${}^{C}Ad_B \in \mathbb{R}^{3\times6}$ is the adjoint transformation matrix transforming twist vectors from frame B to frame C, refer [4] for more details.

We can see that the number of actuators exceeds the chassis center of mass variables that give rise to kinematic redundancy. Various redundancy resolution methods can be used, like pseudo-inverse Jacobian, priority task-based approach, and torque minimization [7]. Many factors make this kinematic model particularly beneficial. It serves as the basis for the kinematic control of the AAW vehicle while preserving pure rolling constraint. The contact velocity $C[{}^{O}V_B]$ has been removed from the equation. Secondly, it is likewise simple to extract the static model, which now connects the contact force acting on the wheel to the torques applied at the joints and all other wrenches used to manipulate the robot [4].

For medium-scale robots or rovers operating at low speeds, kinematic-based motion control may be sufficient, as shown in [8]. As we aim to deploy active articulation in full-scale vehicles operating at high speeds, a dynamic model is needed to handle the link, and wheel inertia and high-torque motors are needed [9]. Additionally, we undertake this kinematic modeling since this would form the basis for subsequent dynamic modeling.

Dynamic Modeling

An AAW vehicle's dynamic model can be broken down into actively articulated links and wheels with rolling constraints. Like legged robots, [10], in AAW vehicles, the links, including the wheels, are coupled to a free-floating base B that serves as the model for the robot. Considering an example in [11] that uses robot ANYmal, an AAW vehicle can be modeled using Lagrangian dynamics with kinematic (including pure rolling) and dynamic constraints. The equation can be formulated as:

$$M(q)\ddot{q} + C(q,\dot{q})\dot{q} + G(q) = S^{\top}\tau + J_C^{\top}\lambda \tag{7}$$

where $M(q) \in \mathbb{R}^{n\times n}$ is the mass matrix, $C(q,\dot{q}) \in \mathbb{R}^{n}$ is the Coriolis matrix, $G(q) \in \mathbb{R}^{n}$ is the gravity vector, $S^{\top} = [0_{n_\tau \times n} I_{n_\tau \times n_\tau}] \in \mathbb{R}^{n_\tau \times n}$ is the selection matrix that represents which joints are actuated [12]. $\tau \in \mathbb{R}^{n}{}_{\tau}$ is the actuated torque vector, $J_C^{\top}\mathbb{R}^{3n_w\times n}$ is the contact Jacobian and $\lambda \in \mathbb{R}^{3nw}$ represents vector of constraint forces. Where n, n_τ and n_w are the total degrees of freedom (chassis position, angular velocities and number of joints), actuated torques and number of wheels, respectively [13].

Research Opportunities

Unified Design and Architecture Selection Framework:

The design and development of an AAW wheeled vehicle involve multiple facets. In Fig. 4 we show a complex framework in which many parameters depend on each other.

After surveying the literature, it can be seen that most of the AAW vehicle's designs and architecture are selected based on intuition. Then control algorithms are implemented to make the system work. An AAW vehicle has numerous modules concerning the integration of performance parameters, control-configured design, software development, and functional requirements (stakeholder needs and project cost). Down-selecting an optimal design (no. of wheels or material) and architecture (serial or parallel linkage) requires consideration of all the facets that themselves have complex interdependencies, as shown in Fig. 4.

A unified framework is needed [14] that automatically integrates all the interdependencies. Like Model-Based Systems Engineering Approach (MBSE) [15] but also connecting different CAD and simulation software that will

FIGURE 4 Unified design framework schematic

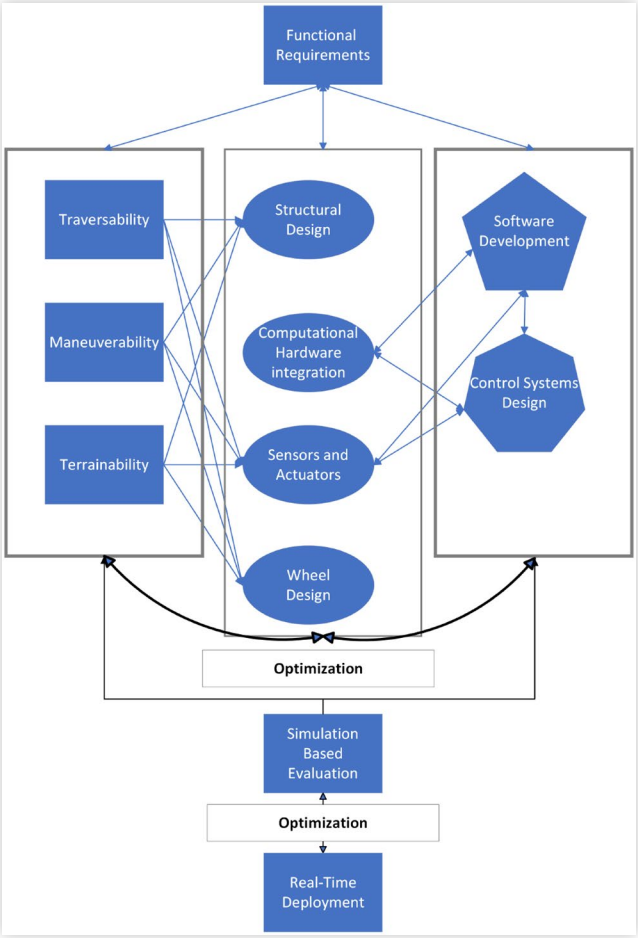

reflect component and sub-system level change and allow for an efficient design and architecture selection.

Integrating Redundancy in Control

Each link in an AAW vehicle can be moved (rotated or translated) using an actuator. The number of actuators (joints) exceeds the variables to be controlled [x y z ϕ θ ψ], it introduces kinematic redundancy within the system. The desired vehicle configuration can be achieved through multiple solutions as shown in Fig. 5. Fig. 5 shows a 12 DOF vehicle similar to Fig. 11. Configuration Space 'C' $\subset R^{12}$ and Task Space 'T' $\subset$ SE(3). This shows that there are more joints than the degrees of freedom needed to control, which introduces kinematic and actuation redundancy [16]. Black lines indicate infinite solutions in which a stable support polygon can be achieved. Also, there is a possibility of high-velocity build-ups within the joints that can cause a non-zero movement at the end effector (wheels), causing motion disturbances that introduce dynamics level redundancies [17].

Fig. 6 shows a standard control framework for an AAW vehicle. Integrating both kinematic and dynamic level redundancies within the motion control framework can yield better

FIGURE 5 Configuration space and task space scenario

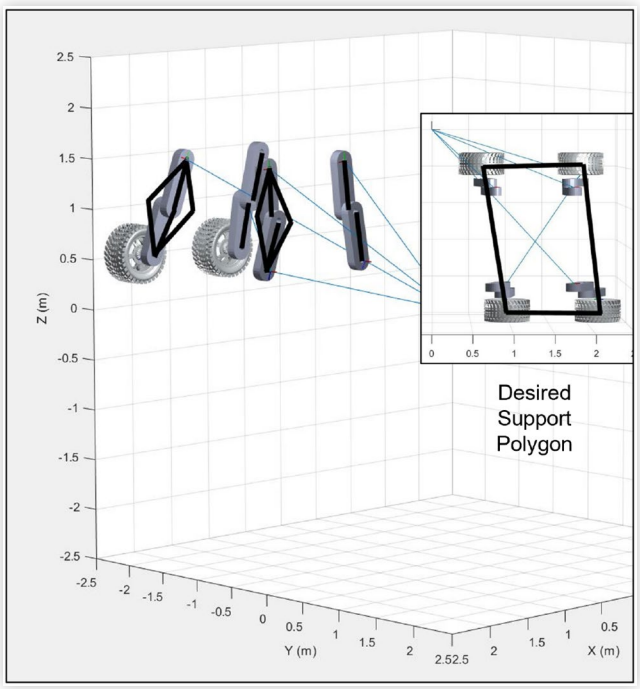

FIGURE 6 Standard AAW vehicle control framework

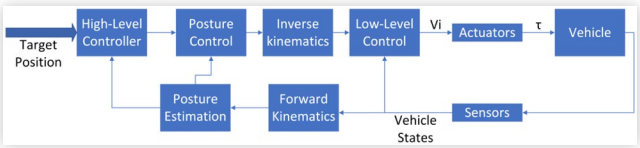

FIGURE 7 Driving with reconfiguration (Multi-Mode) for varying slope configurations

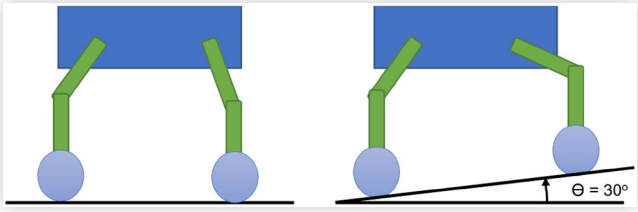

locomotion, minimizing unwanted disturbances and actuator torques, thus increasing efficiency.

Multi-Mode Active Reconfiguration

Most of the platforms in literature except [18, 19] focus on a single locomotion mode active at a time: Either pure driving or pure articulation mode. However, there may be a situation in which simultaneous driving and articulation (hybrid locomotion) is needed to achieve desired performance. Fig. 7 shows two different vehicle configuration on a flat terrain and an inclined terrain. Let's consider a scenario in which a roll angle of zero degrees needs to be maintained along with additional parameters set by the higher level controller like wheelbase, track width, constant velocity and pitch angle. In order to adapt to the terrain without a discontinuity, vehicle needs to achieve the optimal pose while driving (without stopping). This introduces the following two locomotion modes.

Pure Driving Mode

The system's intrinsic mobilities are not utilized in this mode. It is the most effective way of mobility on surfaces without ridges and cracks like a road (in a necessary condition that the leg transmission mechanisms are irreversible or passively blocked) [20].

Driving with Reconfiguration Mode (Multi-Mode)

In this mode, the posture is optimized using internal active mobilities to improve locomotion performance [20]. This style of mobility can be used over uneven terrain without discontinuities, such as sloping land or rocky terrain. Fig. 7 provides a graphic illustration of this position for two slope configurations [20].

Understanding the complex dynamics of different modes remains a challenge and a research opportunity. How one mode's dynamics influence the other will help us develop algorithms that will enhance the performance of an AAW

vehicle that can efficiently adapt to a broad range of terrain conditions.

Motion Control Deployment Opportunities

Motion control of AAW vehicles is crucial to achieving the desired locomotion performance, characterized by carefully defined quantifiable performance metrics. A suitable selection of metrics can now empower deployment in a model- and learning-based settings shown below.

Model-Based Control

Model-based control relies on the kinematic and dynamic models of the system that can be solved efficiently using the following approach.

Whole-Body Model-Predictive Control

AAW vehicles involve a complex control task with kinematics and dynamics of the whole body, including joint movements in the cartesian space, and internal collisions must be avoided. Conventional analytical solutions cannot incorporate inequality constraints and wheel-terrain contact well. Hence, numerical optimization techniques are more desirable for such complex systems [19]. Also, the motion planner must handle significant nonlinearities in the dynamic model of an AAW vehicle. This intricacy makes the optimization issue susceptible to local minima and can make real-time computation challenging. The hierarchical control technique that uses both Model-Predictive Control (MPC) and a Whole-Body Controller (WBC) is beneficial to address these challenges. The idea of using MPC and WBC is to make a robot execute multiple tasks simultaneously [21]. Fig. 8 shows the Whole-Body MPC framework. The MPC would generate the desired motion plan by optimizing joint velocities and ground reaction forces, while the WBC would track the required joint torques for all the joints to achieve the desired motion plan. [18, 11, 22] use some of the well-known platforms that implement the WBC technique. [23] uses WBC with ZMP stability criterion. So a variation of the controller can be seen in the literature based on the specific needs of the platform. MPC is a prevalent method in the robotics community for its capability to handle complex systems with non-linear constraints [24]. MPC is formulated as finding an optimal control input u, in the AAW vehicle case, joint torques over a receding horizon T based on the last state measurement. The current control policy is applied until an updated policy is made available. An example is shown in [18].

FIGURE 8 Whole Body Model-Predictive Control Framework

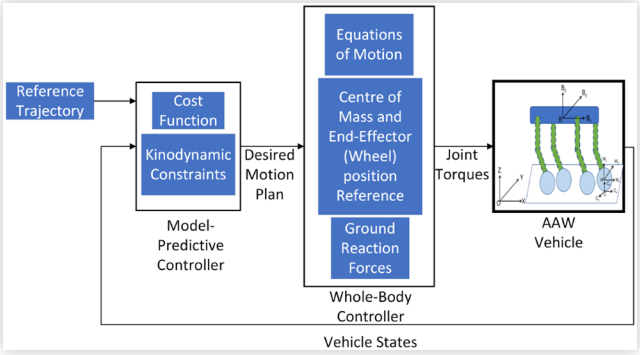

$$minimize\ u(.)\quad \phi\left(x(T)\right)+\int_0^T l\left(x(t),\ u(t),\ t\right)dx \tag{8}$$

$$subjected\ to\ \dot{x}(t)=f\left(x(t),\ u(t),\ t\right) \tag{9}$$

$$x(0)=x_o \tag{10}$$

where Eq.9 and Eq. 10 are kinodynamic constraints applied to the system. Kinodynamic planning is a set of problems in robotics and motion planning where velocity, acceleration, force, or torque limitations, as well as kinematic constraints like avoiding obstacles, must be satisfied [25]. Additional state-input equality and inequality constraints can be applied per the performance requirement. WBC computes optimal generalized accelerations $\dot{u}$ and contact forces $\lambda^{\top}$ based on the desired motion plan. It is formulated as a quadratic problem consisting linear equality and inequality constraints. Formulation is shown below based on [19]:

$$\sum_{i=1}^{n}\frac{\omega_i}{2}\left\|C_iX-e_i\right\|^2 \tag{11}$$

$$s.t\ C_{eq}X=b_{eq} \tag{12}$$

$$b\le BX\le\bar{b} \tag{13}$$

where $\|C_iX-e_i\|^2$ is the cost function, $X=\left[\dot{u}\lambda^{\top}\right]$ and $C_{eq}X = b_{eq}$, $\underline{b}\le BX\le\bar{b}$ are the equality and inequality constraints respectively. Upon computing the optimized solution, the required joint torques can be computed using Eq. 5.

MPC is a computationally expensive controller but with the advent of high compute hardware; such a challenge is minimized. However, MPC requires a carefully formulated system model, which makes it dependent on the model's accuracy. As the AAW vehicle has high DOF, formulating both kinematic and dynamic models is challenging, which may limit the power of MPC. [7].

Priority Task Based Control

The vehicle only sometimes has prior knowledge of off-road terrain and relies on exteroceptive and proprioceptive sense the terrain. Even if the MPC-WBC framework has the required data from the sensors and allows for simultaneous articulation and driving, many component-level control systems are trying to achieve the desired motion plan and satisfy the given constraints. There can be situations where the articulations hit the kinematic limits, or the vehicle may lose stability due to multiple components performing motions. In a complex system like an AAW vehicle, a strict priority needs to be established for an appropriate motion plan. Table 1. shows an example of having priority based motion control approach [11].

Deep Reinforcement Learning-Based Control

To tackle a broad range of terrain adaptability, a more generalized motion control formulation is required that integrates hybrid locomotion mode (pure driving, pure articulation, or multi-mode) for superior locomotion. The system should be more robust to environment uncertainties [26]. This is where Deep Reinforcement Learning or hybrid DRL [27] approaches have shown promising results.

Fig. 9 represents a DRL framework for an AAW vehicle. A control problem is described as a Markov Decision Process (MDP) in the RL framework. The stochastic control process is modeled mathematically using the MDP, which is frequently employed in RL. An agent observes a state $s_t \in S$ from the environment at each timestep and outputs an action $a_t \in A$. The environment then changes into s_{t+1} via the state transition function $p(s_{t+1}|s_t, a_t)$, rewarding the agent with r_t R: A X S → R and resulting in a new observation. A stochastic strategy $a_t|s_t$ parametrized may guide the agent's behavior. Through environmental interactions, RL algorithms update θ to maximize the cumulative discounted rewards $E\left[\sum_{t=k}^{\infty} \gamma^t r_t\right]$ where k is the current time step and γ is the discount factor [26]. [28] describes different methods and policies for the RL problem.

AAW vehicle features complex dynamics and how actions at various time steps affect long-term results. They also have high-dimensional action spaces, which prevent the enumeration of actions using conventional methods, and high-dimensionality and redundant sensory observations. Deep RL holds the promise of providing answers like in [26]. DRL techniques have some drawbacks, including reward sparsity (low-probability reward outcome while randomly exploring consequences of actions), temporal credit assignment (crediting action-decisions made over time given a reward/punishment outcome), data inefficiency (requiring a large number of training samples to obtain a policy), and challenges in learning a task-relevant representation of input data that is crucial for policy learning [29].

TABLE 1 Example of priority based tasks

Priority	Task
1	Chassis equations of motion
2	Kinematic and dynamic limits
3	Nonholonomic rolling constraint
4	Chassis linear and angular motion tracking
5	Articulated suspension motion tracking
6	Non-Articulated suspension motion tracking
7	Contact force minimization

FIGURE 9 Deep Reinforcement Learning Framework

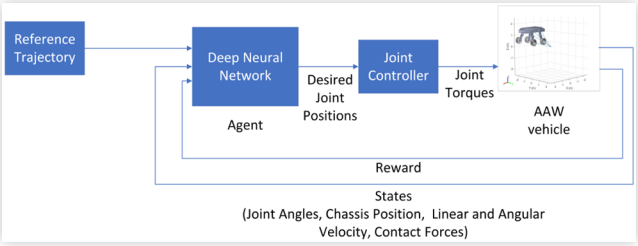

Quantifiable Performance Parameters

An AAW vehicle should have well-defined metrics that measure performance to achieve a global(external) and a local(system) objective. Fig. 10 shows three key performance parameters, each having quantifiable performance measures that could be significant to develop an appropriate design, configuration, planning, and control methods. Performance parameters should relate to an output of the system [30] given the input, like energy usage. Described below are some of the critical parameters that can have a significant impact on locomotion performance. [31] describes all the parameters in greater detail with the formulation.

Traversability

For any AAW vehicle to be driven on uneven terrain, its control and configuration should be able to have efficient traction for it to traverse in diverse conditions [31].

FIGURE 10 Key performance measures

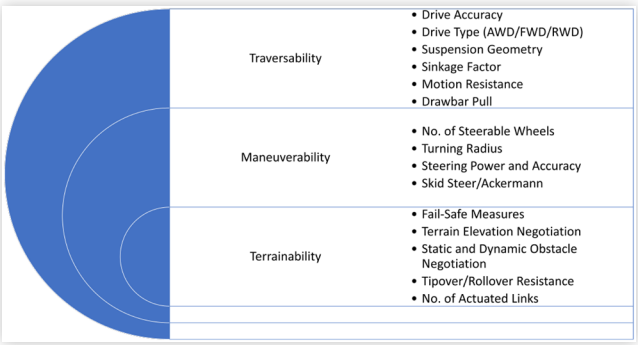

Sinkage Factor

AAW vehicle's wheels can sink while traversing in an off-road environment depending on soil compaction [32]. Maximum sinkage can be defined knowing soil parameters as:

$$z_{rw} = \frac{3W_w cos\theta}{(3-n)\left(k_c + b_w k_\phi\right)\sqrt{d_w}}^{\frac{2}{2n+1}} \quad (14)$$

As a function of the soil parameters n, k_c, k_ϕ, and the wheel dimensions d_w, b_w, this equation depicts robot performance as wheel sinkage [31].

Drawbar Pull

Drawbar pull is the force available to pull or push an extra cargo until the maximum traction is reached. It is the difference between traction and motion resistance [31].

Motion Resistance and Drive Torque

For a vehicle, its internal and external motion resistances need to be accounted for, which defines efficiency and can estimate the total drive torque required to create optimal traction.

Maneuverability

A robot can adjust its direction, avoid hazards, and navigate through congested environments [31]. The type of steering affects maneuverability.

Skid-Steering

Due to the bulldozing and compaction of the terrain, when a robot is skid steering, the lateral motion of the wheels creates a large dissipation of energy. The steering motions are more effective and require less power to execute the motions when the wheel sinkage is reduced [31].

Active Articulation Active articulation significantly increases maneuverability even in weak soil areas, but with it comes the system's increased complexity, which requires careful planning and control.

Ackermann Steering Ackermann steering would have lower energy loss as compared to skid-steering but increases the turning radius which may not be desired in confined spaces.

Terrainability The ability of a vehicle to traverse challenging terrain characteristics without endangering its stability or forward motion is known as terrainability. Terrainability is used to measure the effectiveness of robotic locomotion and is connected to perception and autonomous navigation, whose safe and correct execution depends on the ability of locomotion to deal with or adapt to terrain imperfections [31].

Static Stability The gravitational stability margin, which is the shortest distance between the center of gravity projected on the ground plane and the edge defined by the contact points of two wheels, is used to describe the stability of a wheeled robot that is stationary or moving at a constant pace. The gravitational stability margin is the lateral stability margin if the robot is traveling along a cross-hill slope (or normal to a downhill), and the longitudinal stability margin, if it is traveling parallel to a downhill slope [31].

Gradeability Understanding gradeability in terms of wheel-terrain interaction is essential. A vehicle may have sufficient power to travel varied elevations, but soil compaction could affect soil's ability to resist shear forces caused due to tractive force developed by the tire. Gradeability could also be affected by the tire design.

Zero-Moment Point (ZMP) Stability Criterion

AAW vehicles have internal reconfigurability that shifts the position of their center of mass, inertial, and contact forces. The point where sum of moments due to all the inertia and gravitational forces equals zeros is called a ZMP [33]. Fig. 11 shows an example of a 12 DOF AAWvehicle. The polygon formed by the contact points of the wheels is called a support polygon [34, 35].

It is critical for hybrid locomotion systems to maintain a dynamic balance while some or all of the wheels are in contact. The support polygon of a rigid object in contact with a stationary environment and subject to vertical gravity is the horizontal region in which the center of mass must be located to achieve static stability [36, 37]. From [38], it can be seen that as ZMP reaches the edge of the support polygon, any additional moment outside the support polygon could cause the system to roll about the wheel's edge, leading to instability.

FIGURE 11 ZMP stability criterion

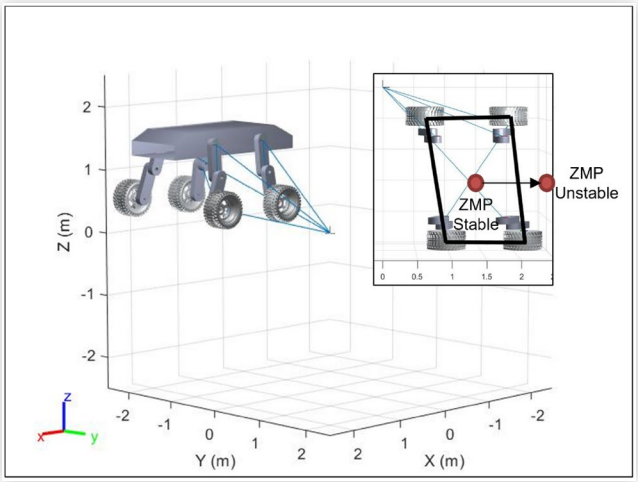

Similarly, to be dynamically stable, the AAW vehicle's ZMP should lie within the support polygon formed by the contact points of the wheels.

Active-Articulation: Initial Case Study To understand one of the advantages of the AAW vehicle, we have considered a test scenario of a Summit-XL robot traversing an uneven terrain using the CoppeliaSim simulator and interfacing it with Matlab. Fig. 12a and Fig. 12b show Summit-XL robots traversing on the terrain without and with articulation, respectively. The desired angle commands are sent from Matlab, which also causes a noisy motion, as shown in Fig. 15. CoppeliaSim uses a PID controller in order to achieve joint position control.

Looking at the scenario above, one of the important performance parameters for traversability is the ability to adapt to the terrain elevation. Minimizing chassis roll will lead to improved stability. Required articulation has been formulated kinematically as shown below

$$\theta = \sin^{-1}\left(\frac{l_w}{2l_l}\tan|\phi|\right) \tag{15}$$

where θ is the required articulation angle, l_w is the length between two wheel joints along the track width, and l_l is the length of the rocker links and ϕ is the body roll angle. Fig. 13 shows the summit-xl robot framework. Vehicle roll information from the simulator is used for calculating the desired articulation angle or joint positions for each rocker arm. Currently, only a proportional controller has been deployed for analyzing advantages of active articulation. Joint torques are computed by the Coppelia Sim simulator that adjust the rocker arm positions accordingly.

The joints get the required articulation angle for minimizing body roll, which could be a performance parameter.

FIGURE 12 Summit-XL robot test scenario

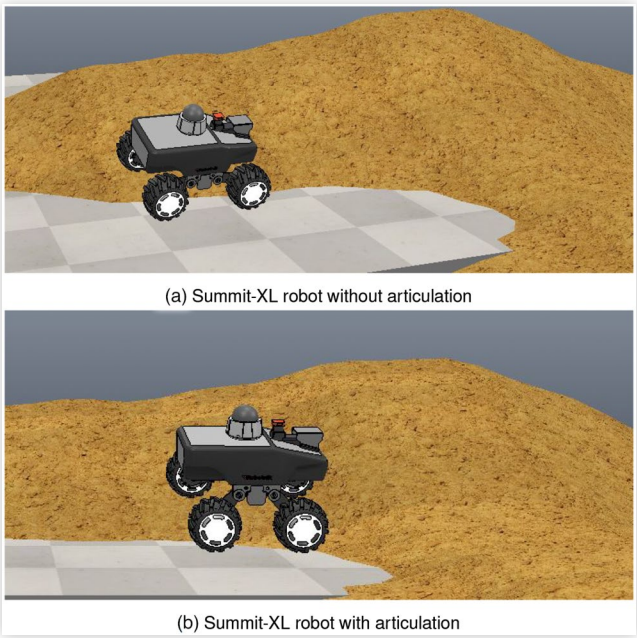

(a) Summit-XL robot without articulation

(b) Summit-XL robot with articulation

FIGURE 13 Summit-XL robot roll minimization framework

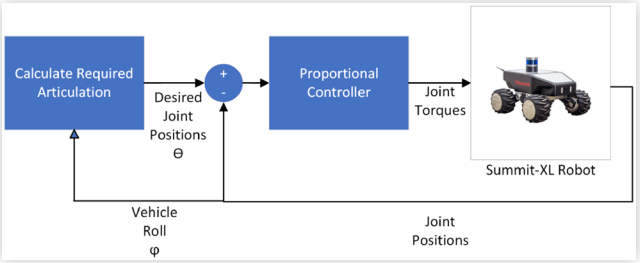

FIGURE 14 Summit-XL robot Arm Angles vs Time Curve

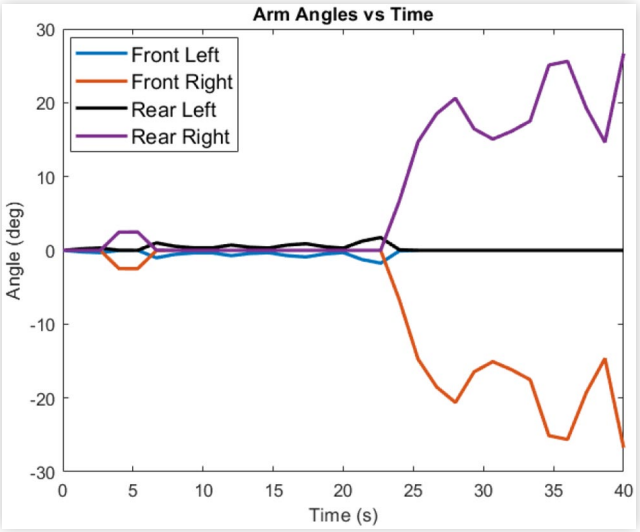

Fig. 14 shows the arm angles vs. the time. The front left and rear left joints are not articulated as they go over the slope. Only the rear right and front right joints articulate, which aids in minimizing roll. As the slope angle for the time does not change for the duration of the simulation, both the front right and rear right joints have similar articulation angles.

Fig. 15 shows the Summit-XL robot's roll vs. time curve.. As observed, while the robot traverses over a slope, the chassis roll is significantly reduced with active articulation compared to no articulation. Such a scenario could be beneficial to maintain dynamic stability when an off-road vehicle is transporting critical equipment.

Active articulation can affect the vehicle's pitch, yaw, desired velocities and vertical accelerations. A high pitch or yaw angle can cause an AAW vehicle to lose stability and control. To maintain balance and navigate effectively, the vehicle's control system must accurately measure and compensate for these angles using sensors and actuators to adjust the position and orientation of the legs and wheels. Fig. 16 and Fig. 17 show the comparison of additional parameters with and without active articulation.

As seen, active articulation reduces the pitch by controlling robot's front right and rear right joints maintaining a level drive. Though, it does not achieve peak linear velocity as the robot's wheels slip along the terrain surface to achieve an optimal pose and causing a change in velocity.

FIGURE 15 Roll vs. Time Curve

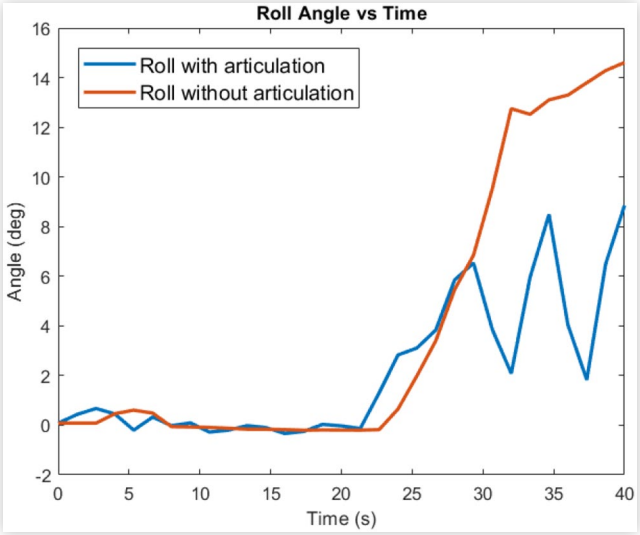

FIGURE 16 Summit-XL robot Euler Angles vs. Time Curve

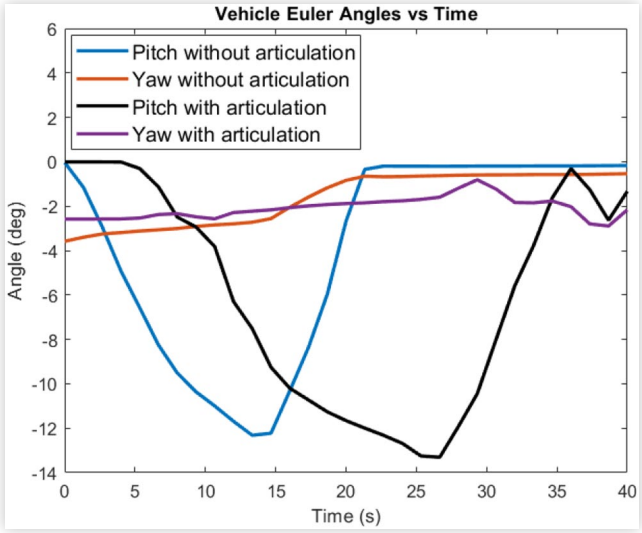

FIGURE 17 Summit-XL Robot Linear Velocity vs. Time Curve

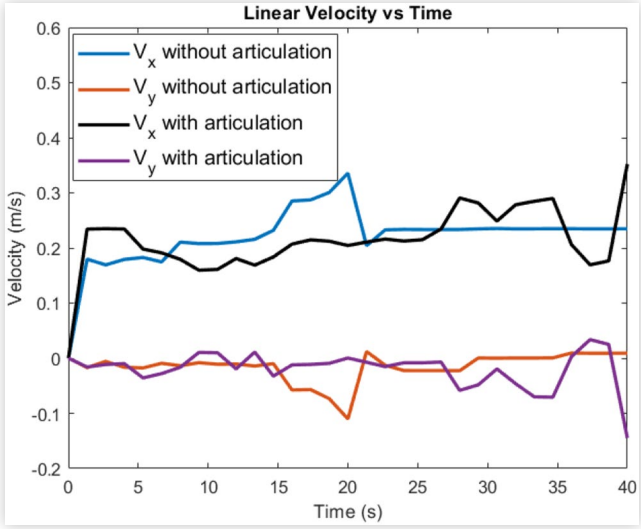

FIGURE 18 Summit-XL Robot Power Consumption vs. Time Curve

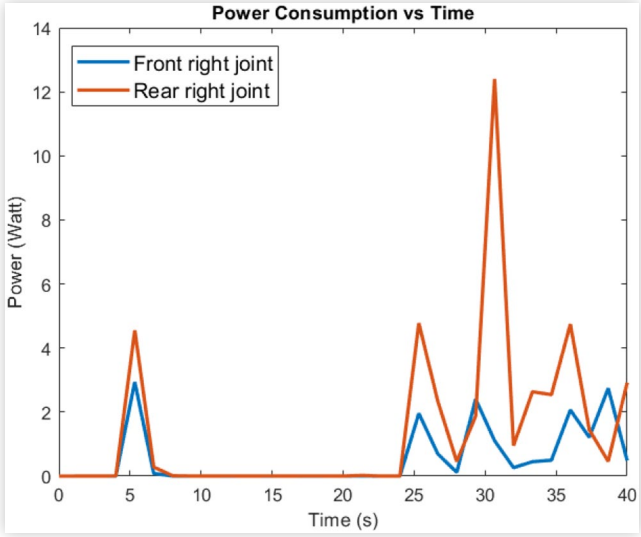

Active articulation requires additional power to operate, which can increase the overall energy consumption of the vehicle. However, it is essential to note that the power consumption of AAW vehicles can vary widely depending on a variety of factors, including the specific design of the vehicle, the type of suspension or articulation system used, and the vehicle's operating conditions. Fig. 18 shows the power consumed by the front right and rear right motors.

Average power consumed by front right motor and, rear right motor is 0.88 Watt and 3.15 Watt, respectively.

Desired locomotion advantages can be achieved based on the performance parameters defined, and with the required sensing, actuation, and computing technology available, AAW vehicle platforms can be efficiently deployed.

Initial Case Study: Limitations

Current formulation of the required articulation angle is based purely on kinematics and does not consider dynamics and obstacle avoidance scenarios. Combining kinematic and dynamic formulation from Eq. 1 and Eq. 7 or using a DRL technique will improve motion control of the robot. Additionally, actuators are considered ideal that assumes the controller has infinite bandwidth and no latency [39]. Incorporating hardware constraints and adding noise within a specified threshold to the states and output torques would achieve a more realistic simulation. Algorithms can perform better in real-time rather than further hand-tuning them to achieve the desired performance.

Conclusion and Future Work

In this paper, AAW vehicle technology development has been discussed. We have reviewed the modeling approaches inspired by the legged and wheeled-legged robot community. AAW vehicle technology was developed in the previous era, but we were limited by the technology of the time. With the current capability of design software, sensing, actuation, and computing technology, faster and more efficient design and development of AAW vehicles could be exercised. AAW vehicles will have a significant advantage over conventional off-road wheeled vehicles.

One of the critical challenges associated with the platform is its complexity due to high DOF. Complex dynamics must be addressed to achieve the most optimal trajectory and reconfiguration. However, with the advent of sophisticated simulation software and deep reinforcement learning methods, tackling the challenges associated with AAW vehicles shows promise and further intriguing research opportunities.

Future work involves developing a 12 DOF vehicular system in simulation and testing it with the model-based and learning-based approaches against performance parameters defined for varied test scenarios.

Contact Information

Dhruv Mehta
dhruvm@clemson.edu

Krishna Chaitanya Kosaraju
kkosara@clemson.edu

Venkat Krovi
vkrovi@clemson.edu

Acknowledgement

This work was supported in part by the US National Science Foundation under NSF IIS-1925500 and NSF CNS-1939058.

References

1. Hornback, P., *The Wheel Versus Track Dilemma in*, (1998).
2. Siegwart, R., Lamon, P., Estier, T., et al., "Innovative Design for Wheeled Locomotion in Rough Terrain," *Robotics and Autonomous Systems*, 40, Intelligent Autonomous Systems - IAS -6, 151-162, 0921-8890, https://www.sciencedirect.com/science/article/pii/S0921889002002403 (2002).
3. Lim, K.B., Park, S., Kim, S.-J., et al., "Behavior Planning of an Unmanned Ground Vehicle with Actively Articulated Suspension to Negotiate Geometric Obstacles," in *2009 IEEE/RSJ International Conference on Intelligent Robots and Systems*, 821-826, (2009).
4. Alamdari, A., Zhou, X., and Krovi, V., *Kinematic Modeling, Analysis and Control of Highly Reconfigurable Articulated Wheeled Vehicles*. Vol. 6 (Aug. 2013)
5. Hidalgo, J., and Cordes, F., *Kinematics Modeling of a Hybrid Wheeled-Leg in*, (2012).
6. Fu, Q., Zhou, X., and Krovi, V., "The Reconfigurable Omnidirectional Articulated Mobile Robot (ROAMeR)," *Springer Tracts in Advanced Robotics* 79 (Jan. 2014).
7. Salzmann, T., Kaufmann, E., Arrizabalaga, J., et al., *Real-Time Neural-MPC: Deep Learning Model Predictive Control for Quadrotors and Agile Robotic Platforms*, 2022, https://arxiv.org/abs/2203.07747.
8. Seegmiller, N., and Wettergreen, D.S., "Control of a Passively Steered Rover Using 3-D Kinematics," in *2011 IEEE/RSJ International Conference on Intelligent Robots and Systems*, 607-612, (2011).
9. Hao, Y., Lu, B., Cao, H., et al., "Run-and-Jump Planning and Control of a Compact Two-Wheeled Legged Robot," *in* in *2022 7th Asia-Pacific Conference on Intelligent Robot Systems (ACIRS)*, (2022), 1-6.
10. Park, H.-W., Wensing, P., and Kim, S., "High-Speed Bounding with the MIT Cheetah 2: Control Design and Experiments," *The International Journal of Robotics Research* 36 (Mar. 2017): 027836491769424.
11. Bjelonic, M., Bellicoso, C.D., de Viragh, Y., et al., "Keep Rollin'—Whole-Body Motion Control and Planning for Wheeled Quadrupedal Robots," *IEEE Robotics and Automation Letters*, 4, 2116-2123, (2019).
12. Dario Bellicoso, C., Gehring, C., Hwangbo, J., et al., "Perception-Less Terrain Adaptation through Whole Body Control and Hierarchical Optimization," *in* in *2016 IEEE-RAS 16th International Conference on Humanoid Robots*, (Humanoids), (2016), 558-564.
13. Al-Shuka, H., Corves, B., and Zhu, W.-H., "Dynamic Modeling of Biped Robot Using Lagrangian and Recursive Newton-Euler Formulations," *International Journal of Computer Applications* 101 (Sept. 2014): 1-8.
14. Goodwin, J., and Winfield, A., *A Unified Design Framework for Mobile Robot Systems in*, (Nov. 2008).
15. Duprez, J., "An MBSE Modeling Approach to Efficiently Address Complex Systems and Scalability," in *INCOSE International Symposium*, 28, 940-954, (July 2018).
16. Fu, Q., and Krovi, V.N., *Articulated Wheeled Robots: Exploiting Reconfigurability and Redundancy*, in (2008).
17. Arai, T., Chiu, S.-h., Saiki, A., and Osumi, H., "Proposal of Dynamic Redundancy in Robot Control," in in *Proceedings of the IEEE/RSJ International Conference on Intelligent Robots and Systems*, 3, (1992), 1921-1926.
18. Bjelonic, M., Grandia, R., Harley, O., et al., "Whole-Body MPC and Online Gait Sequence Generation for Wheeled-Legged Robots," in *2021 IEEE/RSJ International Conference on Intelligent Robots and Systems (IROS)*, 8388-8395, (2021).
19. Sun, J., You, Y., Zhao, X. et al., "Towards More Possibilities: Motion Planning and Control for Hybrid Locomotion of Wheeled-Legged Robots," *IEEE Robotics and Automation Letters* 5 (2020): 3723-3730.

20. Besseron, G., Grand, C., Amar, F. et al., *Locomotion Modes of an Hybrid Wheel-Legged Robot* (Jan. 2004), 825-833, ISBN:978-3-540-22992-6.
21. Eljaik, J., Lober, R., Hoarau, A., and Padois, V., "Optimization-Based Controllers for Robotics Applications (OCRA): The Case of iCub's Whole-Body Control," *Frontiers in Robotics and AI* 5 (Mar. 2018): 24.
22. Kuindersma, S., Deits, R., Fallon, M. et al., "Optimization-Based Locomotion Planning, Estimation, and Control Design for the Atlas Humanoid Robot," *Autonomous Robots* 40 (July 2015).
23. Dario Bellicoso, C., Jenelten, F., Fankhauser, P., et al., "Dynamic Locomotion and Whole-Body Control for Quadrupedal Robots," in *2017 IEEE/RSJ International Conference on Intelligent Robots and Systems (IROS)*, (2017), 3359-3365.
24. Grandia, R., Farshidian, F., Ranftl, R., and Hutter, M., "Feedback MPC for Torque-Controlled Legged Robots," in *2019 IEEE/RSJ International Conference on Intelligent Robots and Systems (IROS)*, (2019), 4730-4737.
25. Donald, B., Xavier, P., Canny, J., and Reif, J., "Kino-Dynamic Motion Planning," *J. ACM*, 40, 1048-1066, 0004-5411, https://doi.org/10.1145/174147.174150, (Nov. 1993).
26. Lee, J., Bjelonic, M., and Hutter, M., in: Cascalho, J.M., Tokhi, M.O., Silva, M.F. et al. (Eds), *Control of Wheeled-Legged Quadrupeds Using Deep Reinforcement Learning in Robotics in Natural Settings*, (Cham: Springer International Publishing, 2023), 119-127, ISBN:978-3-031-15226-9.
27. Joglekar, A., Krovi, V., Brudnak, M., and Smereka, J.M., "Hybrid Reinforcement Learning Based Controller for Autonomous Navigation," in *2022 IEEE 95th Vehicular Technology Conference:* (VTC2022-Spring), (2022), 1-6.
28. Sutton, R.S. and Barto, A.G., *Reinforcement Learning: An Introduction* (Cambridge, MA, USA: MIT Press, 1998). http://www.cs.ualberta.ca/%7Esutton/book/ebook/the-book.html, ISBN:0-262-19398-1.
29. Chen, X., Ghadirzadeh, A., Folkesson, J., et al., "Deep Reinforcement Learning to Acquire Navigation Skills for Wheel-Legged Robots in Complex Environments," in *2018 IEEE/RSJ International Conference on Intelligent Robots and Systems (IROS)*, (2018), 3110-3116.
30. Salvi, A., Buzhardt, J., Tallapragada, P., et al., *Virtual Evaluation of Deep Learning Techniques for Vision- Based Trajectory Tracking in*, (Mar. 2022).
31. Apostolopoulos, D., *Analytical Configuration of Wheeled Robotic Locomotion*, (June 2001).
32. Brecheisen, Z.S., Cook, C.W., Heine, P.R., and de. B. Richter, D., "Micro-Topographic Roughness Analysis (MTRA) Highlights Minimally Eroded Terrain in a Landscape Severely Impacted by Historic Agriculture," *Remote Sensing of Environment*, 222, 78-89, 0034-4257, https://www.sciencedirect.com/science/article/pii/S0034425718305789 (2019).
33. Liu, J., and Veloso, M., "Online ZMP Sampling Search for Biped Walking Planning in *2008 IEEE/RSJ International Conference on Intelligent Robots and Systems*, (2008), 185-190.
34. Hurst, J., Rizzi, A., and Hobbelen, D., *Series Elastic Actuation* (Potential and Pitfalls, Jan. 2004)
35. Vukobratovic, M. and Borovac, B., "Zero-Moment Point - Thirty Five Years of its Life," *I. J. Humanoid Robotics* 1 (Mar. 2004): 157-173.
36. McGhee, R., and Frank, A., "On the Stability Properties of Quadruped Creeping Gaits," *Mathematical Biosciences*, 3, 331-351, 0025-5564, https://www.sciencedirect.com/science/article/pii/0025556468900904 (1968).
37. Bretl, T. and Lall, S., "Testing Static Equilibrium for Legged Robots," *IEEE Transactions on Robotics* 24 (2008): 794-807.
38. Vukobratovic, M. and Borovac, B., "Zero-Moment Point - Thirty Five Years of its Life," *I. J. Humanoid Robotics* 1 (Mar. 2004): 157-173.
39. Hwangbo, J., Lee, J., Dosovitskiy, A., et al., "Learning Agile and Dynamic Motor Skills for Legged Robots," *Science Robotics*, 4, eaau5872, eprint: https://www.science.org/doi/pdf/10.1126/scirobotics.aau5872, https://www.science.org/doi/abs/10.1126/scirobotics.aau5872 (2019).

ISSN 0148-7191